Polymer Chemistry

PAPER

Cite this: *Polym. Chem.*, 2015, **6**, 466

Synthesis and characterization of novel barbwire-like graft polymers poly(ethylene oxide)-*g*-poly(ε-caprolactone)$_4$ by the 'grafting from' strategy

Xinyi Liang,[a,b] Yujie Liu,[a] Jian Huang,[a] Liuhe Wei*[b] and Guowei Wang*[a]

Received 4th September 2014,
Accepted 19th September 2014

DOI: 10.1039/c4py01225a

www.rsc.org/polymers

Novel barbwire-like graft polymers PEO-*g*-PCL$_4$ were synthesized by combination of ring opening polymerization (ROP) and Glaser coupling with thiol–yne addition reaction *via* the "grafting from" strategy. Typically, the precursor (PEO-diyne-PEO)$_s$ of high molecular weight was obtained by Glaser coupling of alkyne-PEO-alkyne, which was prepared by modification of HO-PEO-OH with propargyl bromide. After the diyne groups on PEO were transferred into hydroxyl groups by efficient thiol–yne addition reaction with mercaptoethanol, the macroinitiator [PEO-(OH)$_4$-PEO]$_s$ was obtained and the graft polymers PEO-*g*-PCL$_4$ were synthesized by ROP of ε-caprolactone monomers. The structure of graft polymers was confirmed by GPC, MALDI-TOF MS, ^{1}H NMR, and TGA measurements in detail, and the crystallization behavior of graft polymers was also comprehensively investigated using DSC, WAXD, and POM instruments.

Introduction

In recent years, a variety of polymers with complicated architectures and compositions have been realized by certain synthetic routes *via* the combination of living/controlled polymerization mechanisms and efficient coupling methods. The increasing attention on these complicated architectures is mainly due to their unique physical properties and versatile applications, such as biomedical materials,[1,2] composite materials,[3] nanotechnology,[4] and supra-molecular science.[5] Among these complicated architectures, the graft polymers are synthesized by connecting multiple side chains onto a particular main chain. Usually, for graft polymers, there are many parameters that can be modulated, such as the length, structures and compositions of main chains and side chains, the grafting density and so on. For example, the structures of side chains and main chains of graft polymers can be designed as block,[6] hyper-branched,[7] V-shaped,[8,9] star-shaped,[10,11] dendrimer-like,[12–14] and so on, and the compositions can be chosen from poly(isoprene) (PI),[15,16] poly(ethylene oxide) (PEO),[17] polystyrene (PS),[18–20] poly(acrylic acid) (PAA),[21] poly(hydroxyethyl methacrylate) (PHEMA),[22,23] poly(ε-caprolactone) (PCL),[24] poly(dimethylaminoethyl methacrylate) (PDMAEMA),[25] and so on. With the variations of the above parameters, the graft polymers with certain applications can be easily realized. Importantly, during the synthetic procedure to graft polymers, the designing and synthesizing of main chains are always the key steps. The main chains not only provide controlled grafting sites and grafting density, but also embed the properties of main chains into the final graft polymers. However, in the literature, the length between adjacent grafting sites in graft polymers is always modulated by several monomer units. In such cases, the properties of main chains are always difficult to be discriminated or even can be neglected because of the serious restriction and surrounding of the main chains by side chains.

Alternatively, using the living anionic polymerization and coupling reaction between living species and chlorosilane agent, Mays *et al.* synthesized some novel graft polymers PI-*g*-PS or PS-*g*-PS, in which the grafting sites are separated by PI or PS segments with a certain length.[26–28] After these pioneering studies, by combination of the Williamson reaction, anionic polymerization and living/controlled radical polymerization, Plamper *et al.* also synthesized some similar graft polymers PEO-*g*-PDMAEMA, in which the grafting sites are separated by the PEO segment.[25] Actually, the graft polymers with grafting sites regularly separated by a certain polymeric segment and star-shaped polymers as side chains are rarely reported except for the above two examples. These graft polymers are termed barbwire-like, threaded star-shaped, pearl necklace, multi-graft, centipede or multiple dumbbell polymers, and it can be considered that the cores of star-shaped polymers are sequentially

[a]*State Key Laboratory of Molecular Engineering of Polymers, Department of Macromolecular Science, Fudan University, Shanghai 200433, China. E-mail: gwwang@fudan.edu.cn; Fax: +86 21 6564 0293; Tel: +86 21 6564 3049*
[b]*Zhengzhou Key Laboratory of Elastic Sealing Materials, College of Chemistry and Molecular Engineering, Zhengzhou University, Zhengzhou 450001, PR China. E-mail: weiliuhe@zzu.edu.cn*

linked by a common linear polymer. Because of the existence of main chain segments with a certain length in graft polymers, the properties of main chains could be well expressed in the final graft polymers. For example, from the results of Mays, it was shown that the mechanical properties of barbwire-like polymers can be well controlled by modulating the length of the spaced segment on main chains. However, until recently, the synthesis of the above so-called barbwire-like polymers and the related progress are rather limited and need to be further developed.

On the other hand, from the viewpoint of compositions, PEO is a classical soft segment in multi-constitution polymers, and might endow the polymers with special properties due to its good solubility both in water and organic solvents.[29–31] The polymers containing a PEO segment showed potential applications in high energy density lithium batteries, electronic devices[32] and drug delivery systems.[33] Also, the PCL segment has been extensively used as an important biomaterial for a wide variety of drug delivery carriers and biomedical devices because of its biodegradability and biocompatibility,[34] and as a composite material because of its versatile mechanical properties and miscibility toward some commodity polymers including polyethylene and polypropylene. Thus, the polymers containing PEO or PCL segments are important in theory and applications.

Herein, considering the above progress, we aim to synthesize some novel barbwire-like graft polymers PEO-*g*-PCL_4, in which the grafting sites are specially spaced with a certain length of PEO segments and the PCL segments with controlled lengths are introduced as side chains. In the synthetic route, the ring-opening polymerization (ROP) mechanism, Glaser coupling and thiol–yne addition reaction are well combined (Scheme 1). Furthermore, the crystallization behavior of the graft polymer PEO-*g*-PCL_4 is also investigated.

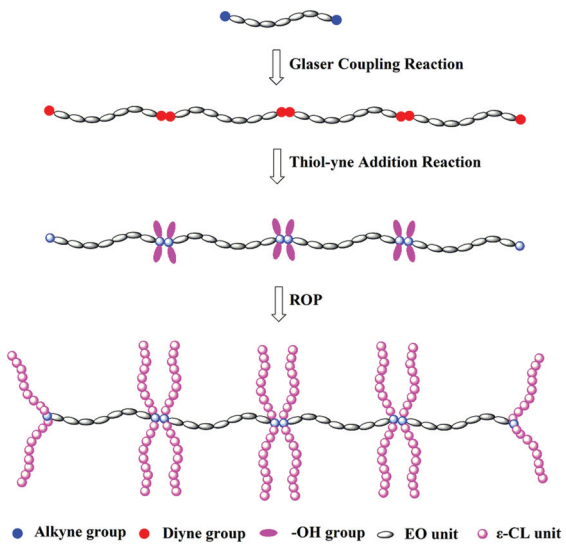

Scheme 1 The illustration of barbwire-like graft polymers PEO-*g*-PCL_4 and the synthetic procedure.

Experimental

Materials

The difunctional HO-PEO-OH was synthesized in our lab according to previous work[35] using ethylene glycol and diphenylmethyl potassium (DPMK) as the co-initiator system. ε-Caprolactone (99%, Aldrich) and propargyl bromide (98%, Aldrich) were purified by distillation from calcium hydride (CaH_2) under reduced pressure and stored at −20 °C before use. Toluene was purified by direct distillation from CaH_2. Tetrahydrofuran (THF, 99%) was refluxed and distilled from potassium naphthalenide solution. Tin(II)bis(2-ethylhexanoate) ($Sn(Oct)_2$, 95%, Sigma) was dissolved in dry toluene (18 mg mL^{-1}). *N*,*N*,*N*′,*N*′,*N*″-Pentamethyldiethylenetriamine (PMDETA, 99%, Aldrich) was used as received. All other reagents and solvents were purchased from Sinopharm Chemical Reagent Co., Ltd (SCR) and used as received except for declaration.

Characterization

The apparent molecular weight of homopolymer PEO was obtained by gel permeation chromatographic (GPC) measurement performed in 0.1 M $NaNO_3$ aqueous solution at 40 °C with an elution rate of 0.5 mL min^{-1} on an Agilent 1100 equipped with a G1310A pump, a G1362A refractive index detector, and a G1315A diode-array detector. Three TSK gel PW columns in series (molecular weight ranges from 0 to 5×10^4 and 5×10^4 to 8×10^6 g mol^{-1}) were calibrated with PEO standards. The absolute molecular weight of homopolymer PEO was performed by GPC measurement through three Waters Styragel columns (pore size 10^2, 10^3 and 10^4 Å), calibrated by narrow polystyrene standards, and equipped with three detectors: a DAWN H ELEOS (14–154°) (Wyatt multiangle laser light scattering detector, He–Ne 632.8 nm), ViscoStar (Wyatt), and Optilab rEX (Wyatt). THF was used as the eluent at a flow rate of 1.0 mL min^{-1} at 35 °C. GPC measurement of graft polymers PEO-*g*-PCL_4 was carried out at 35 °C using LiBr-added DMF ([LiBr] = 15 mM) as the eluent with a flow rate of 1.0 mL min^{-1}. The system was calibrated with linear PMMA standards. ^{1}H NMR and ^{13}C NMR spectra were recorded on a Bruker (500 MHz) spectrometer in $CDCl_3$ solvent with tetramethylsilane (TMS) as internal reference. The matrix-assisted laser desorption/ionization time-of-flight mass spectroscopy (MALDI-TOF MS) measurement was performed using a Perspective Biosystem Voyager-DESTR MALDI-TOF MS (PE Applied Biosystems, Framingham, MA). Matrix solution of dithranol (20 mg mL^{-1}), polymer (10 mg mL^{-1}) and a cationizing salt of sodium trifluoroacetate (10 mg mL^{-1}) in THF were mixed in the ratio of matrix–cationizing salt–polymer = 10 : 1 : 2, and 0.8 μL of mixed solution was deposited on the sample holder. The differential scanning calorimetry (DSC) analysis was carried out on a DSC Q2000 thermal analysis system (Shimadzu, Japan). Samples were first heated from −20 to 120 °C at a heating rate of 10 °C min^{-1} under a nitrogen atmosphere, then cooled to −20 °C at −10 °C min^{-1} after stopping at 120 °C for 3 min, and finally heated to 120 °C at 10 °C min^{-1} after stopping at −20 °C for 3 min. The thermal gravimetric analysis (TGA) curves were

obtained using a Perkin Elmer Pyris 1 at a heating rate of 10 °C min^{-1} under a nitrogen atmosphere. X-ray diffraction (XRD) measurements were carried out using an XPert PRO (PANalytical) with Cu-Kα (1.541 Å) radiation (40 kV, 40 mA). Samples were exposed at a scanning rate of 2θ = 5 °C min^{-1} between 2θ values of 10° and 30°. Crystal growth was observed under a polarized optical microscope (POM, Leica, DM 2500P).

Synthesis of functional PEO with two terminal alkyne groups (alkyne-PEO-alkyne) by propargylation

The functional alkyne-PEO-alkyne was synthesized by modification of HO-PEO-OH with propargyl bromide. First, HO-PEO-OH (3800 g mol^{-1}, 15.00 g, 3.95 mmol) was added into a 500 mL round bottom flask and dried by azeotropic distillation with toluene. After the HO-PEO-OH was dissolved in dry THF (200 mL), sodium hydride (NaH, 2.00 g, 83.30 mmol) was added. Then the ampoule was placed in an ice bath, propargyl bromide (9.20 mL, 126.00 mmol) was added dropwise for 2.0 h and the reaction was continued for another 22 h at room temperature. Finally, the THF solvent was removed by rotary evaporation, and the product was extracted with CH_2Cl_2, and then the organic layer was dried over $MgSO_4$ before purification by precipitation into anhydrous ethyl ether for three times. The obtained alkyne-PEO-alkyne was dried under vacuum at 45 °C for 24 h. ^{1}H NMR ($CDCl_3$) δ (ppm): 3.50–3.75 (–OC***H***$_2$C***H***$_2$O–), 4.20 (–OC***H***$_2$C≡CH), 2.45 (–C≡***CH***). ^{13}C NMR ($CDCl_3$) δ (ppm): 58.4 (–O***C***H$_2$C≡CH), 70.5 (–O***C***H$_2$***C***H$_2$–), 77.1 (–***C***≡CH), 79.6 (–C≡***C***H). $M_{n(NMR)}$ = 5000 g mol^{-1}, $M_{n(MALDI\text{-}TOF\ MS)}$ = 4600 g mol^{-1}. $M_{n(GPC)}$ = 3800 g mol^{-1}, PDI = 1.20.

Synthesis of the precursor (PEO-diyne-PEO)$_s$ containing diyne groups by Glaser coupling reaction

Typically, alkyne-PEO-alkyne (10.00 g, 2.56 mmol), pyridine (400 mL), CuBr (0.74 g, 5.12 mmol), and PMDETA (1.00 mL, 5.12 mmol) were sequentially added into a 500 mL round bottom flask. The system proceeded at room temperature under an air atmosphere for five days. Finally, the solution was concentrated and the crude products were purified by passing them through a neutral alumina column using CH_2Cl_2 as the eluent to remove the copper catalyst. After the product was recovered by precipitation into anhydrous ethyl ether, the obtained (PEO-diyne-PEO)$_s$ was dried under vacuum at 45 °C for 24 h. ^{1}H NMR ($CDCl_3$) δ (ppm): 3.50–3.75 (–OC***H***$_2$C***H***$_2$O–), 4.20 (–OC***H***$_2$C≡C–). ^{13}C NMR ($CDCl_3$) δ (ppm): 58.4 (–O***C***H$_2$C≡CH), 70.5 (–O***C***H$_2$***C***H$_2$–, –***C***≡***C***–,). $M_{n(GPC)}$ = 33 000 g mol^{-1}, PDI = 1.52, $M_{w,\ MALLS}$ = 58 200 g mol^{-1}.

Synthesis of the macroinitiator [PEO-(OH)$_4$-PEO]$_s$ by thiol–yne addition reaction

The macroinitiator [PEO-(OH)$_4$-PEO]$_s$ was obtained by thiol–yne addition reaction between (PEO-diyne-PEO)$_s$ and mercaptoethanol. In a typical example, (PEO-diyne-PEO)$_s$ (2.00 g, 1.00 mmol alkyne groups), 2,2-dimethoxy-2-phenylacetophenone (DMPA) (10.00 mg, 0.04 mmol), mercaptoethanol (2.00 mL, 27.00 mmol) and 40 mL DMF were added into a 50 mL quartz glass vial and degassed by purging with nitrogen for 3.0 min. Then, the system was irradiated with UV (254 nm) for 24 h. After the evaporation of DMF solvent under reduced pressure, the crude product was re-dissolved in CH_2Cl_2 and precipitated into anhydrous ethyl ether for three times, and the obtained [PEO-(OH)$_4$-PEO]$_s$ was dried under vacuum at 45 °C for 24 h. ^{1}H NMR ($CDCl_3$) δ (ppm): 3.50–3.75 (–OC***H***$_2$C***H***$_2$O–), 3.90–3.92 (HO***CH***$_2$CH$_2$–), 2.88 (–S***CH***$_2$CH$_2$–). ^{13}C NMR ($CDCl_3$) δ (ppm): 32.3 (–S***C***H$_2$CH$_2$OH), 45.2 (–OCH$_2$***C***-(–S–)***C***(–S–)–), 62.6 (–SCH$_2$***C***H$_2$OH), 70.5 (–O***C***H$_2$***C***H$_2$–, –O***C***H$_2$C-(–S–)C(–S–)–). $M_{n(GPC)}$ = 33 000 g mol^{-1}, PDI = 2.65.

Synthesis of barbwire-like graft polymers PEO-*g*-PCL$_4$ by the ROP mechanism

By the ROP mechanism, the graft polymer PEO-*g*-PCL$_4$ was obtained using [PEO-(OH)$_4$-PEO]$_s$ as the macroinitiator. The [PEO-(OH)$_4$-PEO]$_s$ (0.50 g, 0.5 mmol hydroxyl groups) dried by azeotropic distillation with toluene, freshly distilled ε-CL (2.0 mL, 0.018 mol) and Sn(Oct)$_2$ solution (5.0 mL, 0.25 mmol, 0.5 equiv. with respect to the hydroxyl groups) were sequentially added into a 100 mL ampoule. After three freeze–thaw cycles at the temperature of liquid nitrogen, the system was charged with nitrogen and the reaction was performed at 110 °C for 12 h. The final graft polymer (PEO-*g*-PCL$_2$) was obtained by direct precipitation into petroleum ether (30–60 °C) and dried under vacuum at 45 °C for 24 h. ^{1}H NMR ($CDCl_3$) δ (ppm): 1.20–1.65 (–C***H***$_2$C***H***$_2$C***H***$_2$CH$_2$C(=O)O– on the PCL segment), 2.20–2.41 (–C***H***$_2$C(=O)O– on PCL), 3.55–3.95 (–C***H***$_2$C***H***$_2$O– on the PEO segment), 3.96–4.13 (–C***H***$_2$OC(=O)– on the PCL segment). $M_{n(NMR),\ PEO\text{-}g\text{-}PCL_4}$ = 477 000 g mol^{-1}. $M_{n(GPC),\ (PEO\text{-}g\text{-}PCL_4)}$ = 88 000 g mol^{-1}, PDI = 2.25.

Results and discussion

Synthesis and characterization of the macroinitiator [PEO-(OH)$_4$-PEO]$_s$

The macroinitiator [PEO-(OH)$_4$-PEO]$_s$ with high molecular weight and controlled functional groups was obtained by sequential propargylation reaction, Glaser coupling reaction and thiol–yne addition reaction (Scheme 2).

The functional alkyne-PEO-alkyne was first prepared by end group transformation of HO-PEO-OH with propargyl bromide in the presence of NaH. As shown in our previous work[36] or literature,[37] this system could give the polymer with high efficiency of functionalization. From the ^{1}H NMR spectrum of alkyne-PEO-alkyne (Fig. 1), except for the resonance signals of protons (–O***C***H$_2$***C***H$_2$–) detected at 3.50–3.75 ppm, the characteristic resonance signals attributed to alkynyl protons (–C≡C***H***) and methylene protons (–OC***H***$_2$C≡CH) on the propargyl group were discriminated at 2.44 and 4.21 ppm, respectively. From the ^{13}C NMR spectrum of alkyne-PEO-alkyne (Fig. 5), the resonance signals of carbons (–C≡***C***H) and (–O***C***H$_2$C≡CH) were detected at 79.6 ppm and 58.4 ppm, respectively, and the signals corresponding to carbons (–O***C***H$_2$***C***H$_2$–) were detected at 70.5 ppm. However, the signal of carbon (–***C***≡CH) was overlapped with that of $CDCl_3$ at

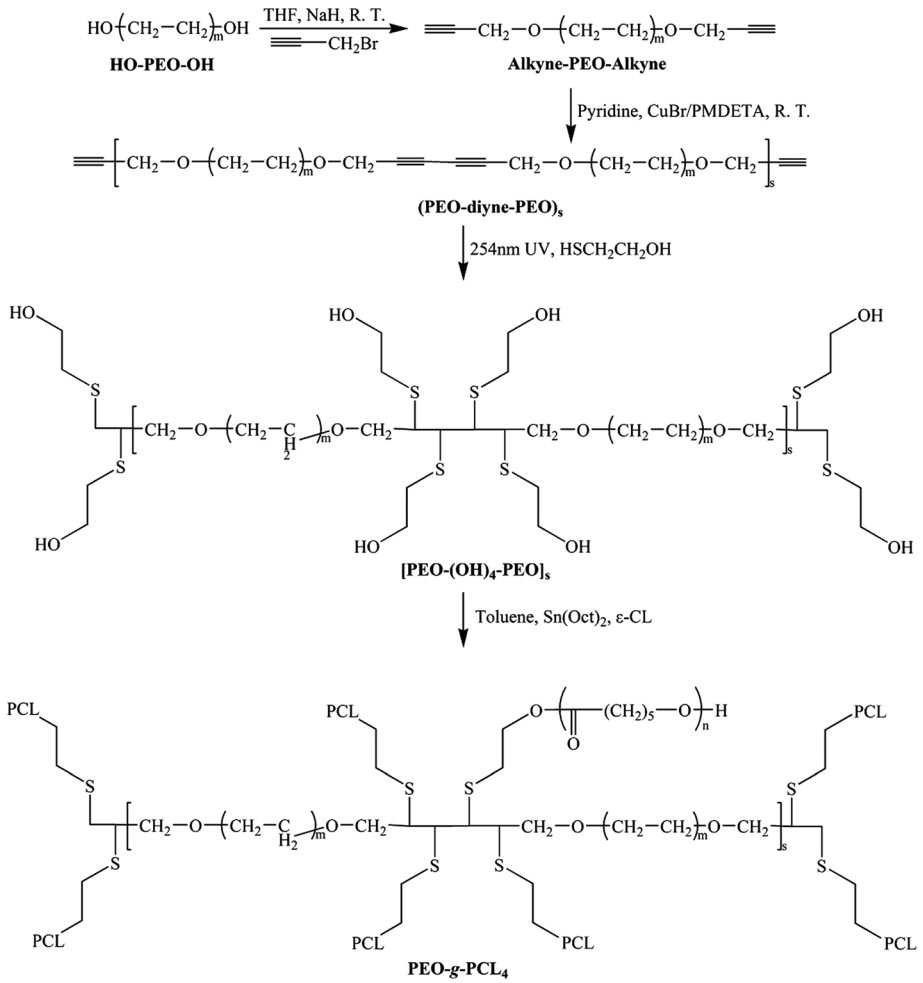

Scheme 2 The synthetic procedure of barbwire-like graft polymers PEO-*g*-PCL_4 and their precursors.

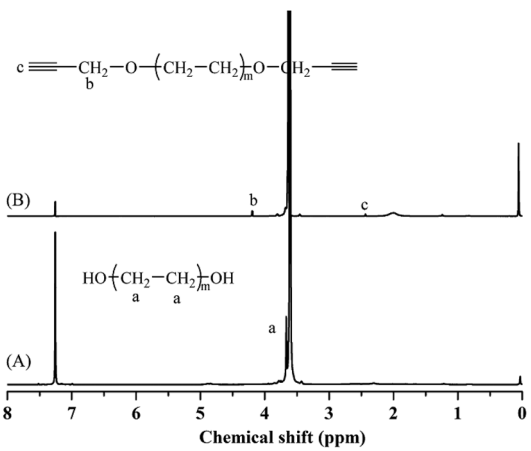

Fig. 1 The ^{1}H NMR spectra of HO-PEO-OH (A) and alkyne-PEO-alkyne (B) (in $CDCl_3$).

77.1 ppm and could not be discriminated. Also, the MALDI-TOF MS was another versatile measurement to characterize the functionalization of polymers. Fig. 2 shows the MALDI-TOF MS of HO-PEO-OH and the corresponding alkyne-PEO-alkyne. Both the mass spectra of HO-PEO-OH and alkyne-PEO-alkyne presented the uniform series of peaks spaced with EO units (44.4 Da). Theoretically, the series of molecular masses for HO-PEO-OH can be expressed as equation: $M_W = M_R + 44.0 \times n + 23.0$, and that for alkyne-PEO-alkyne can be expressed as equation: $M_W = M_R + 44.0 \times n + (39.0–1.0) \times 2 + 23.0$, where M_R denoted the molecular weight of the initiator residue, and 44.0, 39.0, 23.0 and 1.0 were the masses of the EO monomer unit, the introduced propargyl group, the sodium ion and a proton, respectively. Obviously, the *m*/*z* difference between peaks of HO-PEO-OH with the corresponding peaks of alkyne-PEO-alkyne should be equal to 76.0. From Fig. 2, for example, there was an *m*/*z* difference of 76.3 from peak 4568.3 to that of 4644.6, which was rather close to the calculated value of 76.0. Thus, the MALDI-TOF MS further confirmed that the successful modification of PEO ends, and the high efficiency of functionalization of PEO ends would be the prerequisite to the following high molecular weight of the precursor $(PEO\text{-}diyne\text{-}PEO)_s$.

For the precursor $(PEO\text{-}diyne\text{-}PEO)_s$, the efficient Glaser coupling reaction was adopted. Actually, the Glaser coupling between alkyne–alkyne groups has been widely used in organic chemistry,[38] and very recently, this reaction was also

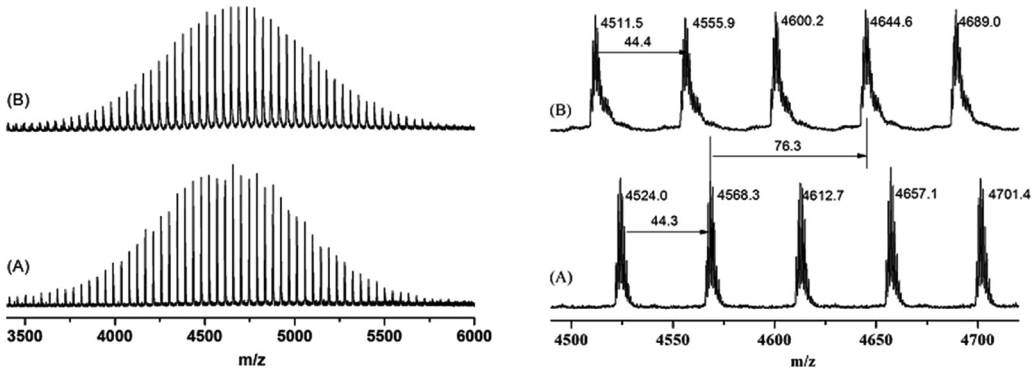

Fig. 2 The MALDI-TOF MS of HO-PEO-OH (A) and alkyne-PEO-alkyne (B).

employed in the preparation of various polymeric structures.[39–42] In our previous work, we found that the 1,3-diynes were produced using terminal alkynes and the CuBr/PMDETA catalyst system with good yields at room temperature and under an air atmosphere.[43] Based on this efficient reaction, various cyclic polymers have been successfully synthesized with high cyclization efficiency (close to 100%).[44–50] Herein, the linear PEO with high molecular weight was also achieved using this Glaser coupling reaction. The GPC trace of the coupled product is shown in Fig. 3. Different from the ^{1}H NMR spectrum of alkyne-PEO-alkyne (Fig. 1), there was almost no obvious change except that the signal of alkynyl protons (–C≡C***H***) at 2.44 disappeared for the ^{1}H NMR spectrum of (PEO-diyne-PEO)$_s$ (Fig. 4). Also, compared with the ^{13}C NMR spectrum of alkyne-PEO-alkyne (Fig. 5), the resonance signal of carbon (–C≡***C***H) at 79.6 ppm was shifted to 70.5 ppm (–C≡***C***–) and overlapped with those on the PEO main chain in the ^{13}C NMR spectrum of (PEO-diyne-PEO)$_s$. Both the NMR spectra comprehensively confirmed the happening of the Glaser coupling reaction. According to the absolute molecular weight of (PEO-diyne-PEO)$_s$ obtained by GPC measurement equipped with a multi-angle laser light scattering detector, the degree of Glaser (DG) coupling reaction could be calculated. As shown in Table 1, the DG was decreased with the increase of the molecular weight of the precursor HO-PEO-OH.

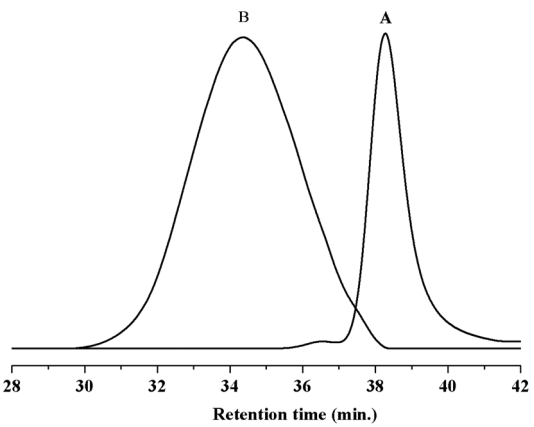

Fig. 3 The GPC traces of HO-PEO-OH (A, M_n = 3800 g mol^{-1}, PDI = 1.20) and (PEO-diyne-PEO)$_s$ (B, M_n = 33 000 g mol^{-1}, PDI = 1.52) (in H_2O eluent).

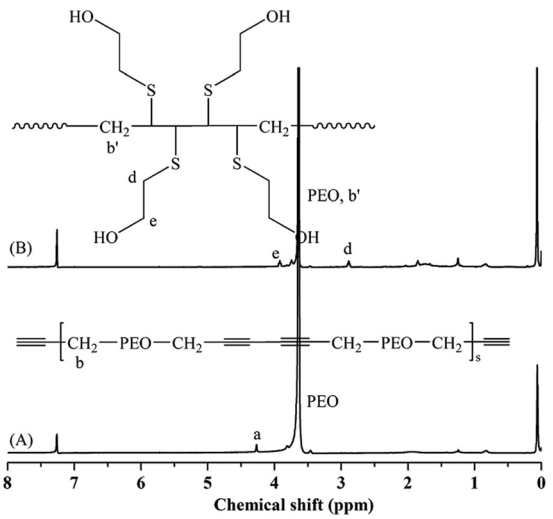

Fig. 4 The ^{1}H NMR spectra of (PEO-diyne-PEO)$_s$ (A) and [PEO-(OH)$_4$-PEO]$_s$ (B) (in $CDCl_3$).

Subsequently, the macroinitiator [PEO-(OH)$_4$-PEO]$_s$ was obtained by another efficient thiol–yne addition reaction between 1,3-diyne structures and excess mercaptoethanol, in which the DMF was used as the solvent and DMPA was used as the photoinitiator under 254 nm UV irradiation. In the literature,[51–55] the thiol–yne reaction usually happened on the terminal alkyne groups under 365 nm UV irradiation, and rarely was work reported on the 1,3-diyne structures. In this work, we found that no reaction happened on 1,3-diyne when 365 nm UV irradiation was adopted; however, this reaction could be carried out smoothly under higher irradiation energy (254 nm UV). From the ^{1}H NMR spectrum of [PEO-(OH)$_4$-PEO]$_s$ (Fig. 4), the characteristic resonance signal attributed to methylene protons (–OC***H***$_2$C≡CH) connected to the triple bonds disappeared completely. Furthermore, the ^{13}C NMR spectrum in Fig. 5 also gives the information that the thiol–yne addition reaction was successful. The resonance signals of carbon (–O***C***H$_2$C≡C–) at 58.4 ppm were shifted to 70.5 ppm (–O***C***H$_2$C(–S–)C(–S–)–) and overlapped with those on the PEO

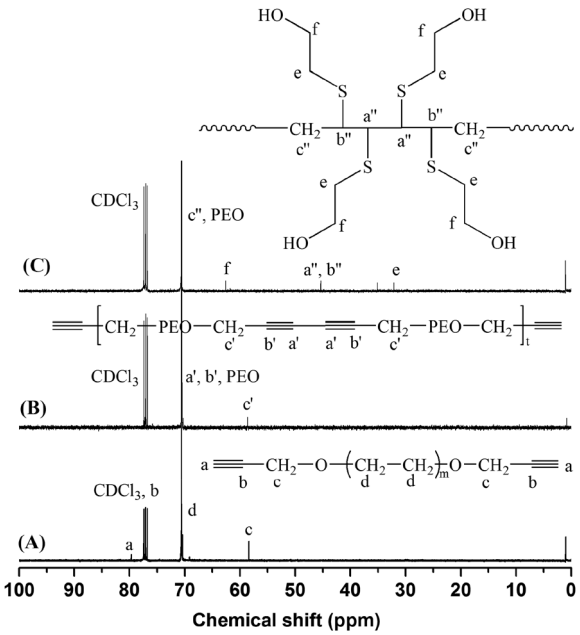

Fig. 5 The ^{13}C NMR spectra of alkyne-PEO-alkyne (A), (PEO-diyne-PEO)$_s$ (B) and [PEO-(OH)$_4$-PEO]$_s$ (C) (in $CDCl_3$).

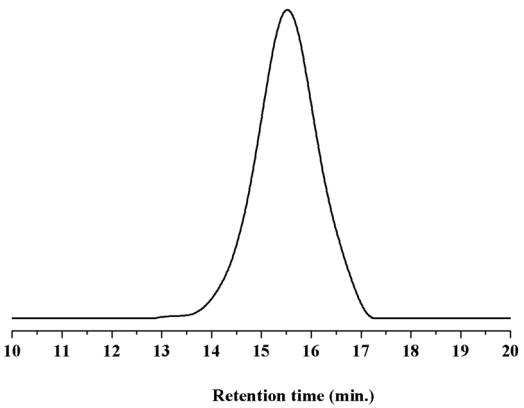

Fig. 6 The GPC trace of graft polymers PEO-*g*-PCL$_4$ (in DMF eluent).

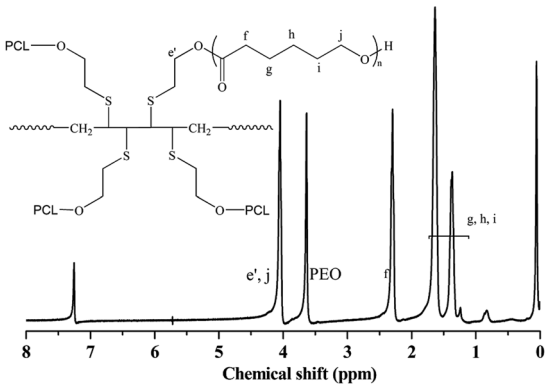

Fig. 7 The ^1H NMR spectrum of graft polymers PEO-*g*-PCL$_4$ (in $CDCl_3$).

main chain, and the signals of carbons on introduced groups (–S***C***H$_2$***C***H$_2$OH) were also detected at 32.3 ppm and 62.6 ppm, respectively. Thus, the results from NMR spectra actually confirmed that each 1,3-diyne had been successfully transformed into hydroxyl groups.

Synthesis and characterization of barbwire-like graft polymers PEO-*g*-PCL$_4$

Using the above [PEO-(OH)$_4$-PEO]$_s$ as the macroinitiator and Sn(Oct)$_2$ as the catalyst, the PCL side chains were introduced onto the PEO main chain by the "grafting from" strategy (Scheme 2). Typically, because the Sn(Oct)$_2$ could react fast with hydroxyl groups to form tin(II) alkoxide initiating species reversibly, the ROP of ε-CL monomers can proceed in a living style.[56] The GPC result of the graft polymer PEO-*g*-PCL$_4$ is shown in Fig. 6, which gives a monomodal peak. Fig. 7 shows the typical ^1H NMR spectrum of PEO-*g*-PCL$_4$, besides the characteristic resonance signals at 3.55–3.95 ppm (–C***H$_2$***C***H$_2$***O–) for the PEO segment, the appearance of the resonance signals at 2.20–2.41 ppm (–C***H$_2$***C(=O)O–) and 3.96–4.13 ppm (–C***H$_2$***OC(=O)–) for the PCL segment confirms that the synthetic procedure of PEO-*g*-PCL was successful. According to the ^1H NMR spectrum, the weight percentage ($W_{NMR,\ PCL}$%) of the introduced PCL segment can be evaluated by eqn (1) (Table 2):

$$W_{NMR,PCL}\% = \frac{(A_f/2) \times 114}{(A_a/4) \times 44 + (A_f/2) \times 114} \times 100\% \quad (1)$$

where A_a and A_f are the integral area of resonance signals at 3.55–3.95 ppm and 2.20–2.41 ppm, respectively. The values of

Table 1 Data for (PEO-diyne-PEO)$_s$ and their precursors

Entry	Samples	$M_{n,\ GPC}$[a] (g mol^{-1})	PDI[a]	$M_{n,\ MALDI\text{-}TOF\ MS}$[b] (g mol^{-1})	$M_{w,\ MALLS}$[c] (g mol^{-1})	DG (degree of Glaser coupling reaction)[d]
I	HO-PEO-OH	1800	1.09	2300		
	(PEO-diyne-PEO)$_s$	48 000	1.32		69 800	30
II	HO-PEO-OH	3800	1.20	4600		
	(PEO-diyne-PEO)$_s$	33 000	1.52		58 200	13
III	HO-PEO-OH	5500	1.09	6000		
	(PEO-diyne-PEO)$_s$	31 500	1.75		51 800	9

[a] Determined by GPC using PEO as the standard and H_2O as the eluent. [b] Determined by MALDI-TOF MS measurement. [c] Determined by GPC equipped with the multi-angle laser light scattering detector. [d] Determined by the formula: DG = $M_{w,\ MALLS,\ (PEO\text{-}diyne\text{-}PEO)_s}/M_{n,\ MALDI\text{-}TOF\ MS,\ HO\text{-}PEO\text{-}OH}$.

Table 2 Data for graft polymers PEO-*g*-PCL_4 and their precursor

Entry	$M_{n,GPC}$[a] (g mol^{-1})	PDI[a]	$W_{NMR,CL}$[c] (%)	$W_{TGA,CL}$[d] (%)	T_m[e] (°C) PEO	T_m[e] (°C) PCL	T_c[f] (°C) PEO	T_c[f] (°C) PCL
$[PEO\text{-}(OH)_4\text{-}PEO]_s$[b]					56.69		41.91	
PEO-*g*-PCL_4 (**1**)	40 000	2.58	50.9	51.2	47.45		28.16	
PEO-*g*-PCL_4 (**2**)	93 000	2.18	68.5	67.3	34.70	54.96	7.41	30.70
PEO-*g*-PCL_4 (**3**)	88 000	2.25	83.5	85.2		56.00		33.13

[a] Determined by GPC using PMMA as the standard and DMF as the eluent for graft polymers. [b] The precursor of $[PEO\text{-}(OH)_4\text{-}PEO]_s$ was exemplified as entry II in Table 1. [c] Calculated from eqn (1) according to ^{1}H NMR spectra. [d] Calculated according to TGA curves. [e] T_m denotes the melting point of PEO or PCL segments in the second heating run. [f] T_c denotes the crystallization temperature of PEO or PCL segments in the cooling run.

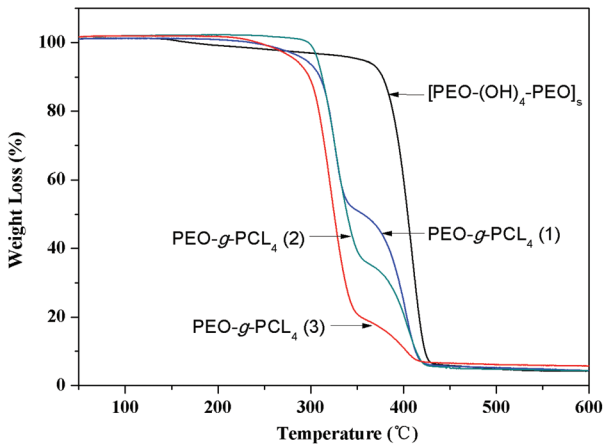

Fig. 8 TGA curves (10 °C min^{-1}) of macroinitiator $[PEO\text{-}(OH)_4\text{-}PEO]_s$ and the graft polymer PEO-*g*-PCL_4 under N_2 atmosphere.

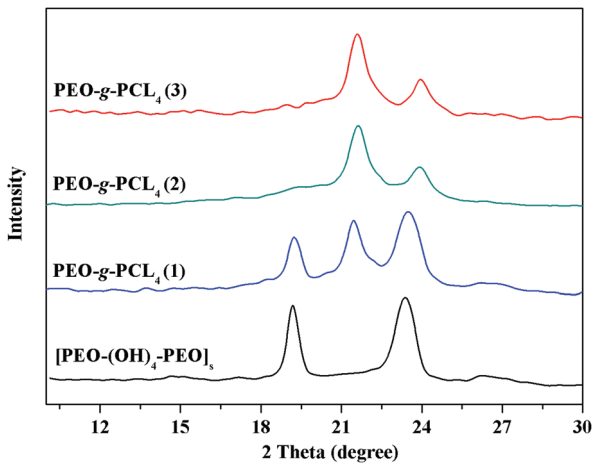

Fig. 9 XRD patterns of graft polymers PEO-*g*-PCL_4.

114 and 44 are the molecular weights of ε-CL and EO monomer units, respectively.

Alternatively, because the PEO and PCL segments could be decomposed at different temperatures, the accurate compositions of PEO and PCL segments in graft polymers could also be well evaluated by TGA measurement. From Fig. 8, we can observe that the macroinitiator $[PEO\text{-}(OH)_4\text{-}PEO]_s$ decomposed at 400 °C. When PCL segments were introduced into graft polymers, the first stage appearing at 330 °C was ascribed to the decomposition of the PCL segment, while the second stage appearing at 390 °C was ascribed to that of the PEO segment. In all TGA curves, these two stages all have an obvious inflection point and the weight percentage ($W_{TGA,PCL}$%) of introduced PCL segments could be well discriminated (Table 2). The obtained values were all rather coincided with that of the corresponding $W_{NMR,PCL}$%.

Investigation on crystallization behavior of graft polymers PEO-*g*-PCL_4

Typically, the PEO and PCL segments are all characteristic crystalline and biodegradable polymers, which had been well studied in the literature.[57,58] For crystalline polymers, the crystallization behavior would seriously affect their biodegradability.[59–61] Thus, in this contribution, the crystallization behavior of this novel barbwire-like graft copolymers PEO-*g*-PCL_4 was also well investigated using XRD, DSC and POM instruments.

First, the XRD instrument was a very efficient method to determine the crystalline structure of polymers. According to the literature, the linear PCL showed two intensive diffraction peaks at 21.6° and 23.9°,[62,63] and the linear PEO showed two intensive diffraction peaks at 19.1° and 23.3°, respectively.[64] Also, the architecture of polymers had almost no effect on their diffraction peaks in XRD measurement. Thus, from the XRD patterns, we could easily determine the crystalline compositions of graft polymers. From Fig. 9, we can observe that, for the marcoinitiator $[PEO\text{-}(OH)_4\text{-}PEO]_s$, the characteristic diffraction peak corresponding to the PEO crystallite could be discriminated at 19.1°. When PCL segments were grafted onto the PEO main chain (PEO-*g*-PCL_4 (**1**)), besides the diffraction peak at 19.1°, a new characteristic diffraction peak corresponding to the PCL crystal also appeared at 21.6°, which confirmed that both PEO and PCL were crystallized. With the increase of the PCL content, in the samples PEO-*g*-PCL_4 (**2**) and PEO-*g*-PCL_4 (**3**), the signals to the PEO crystal could no longer be discriminated, while the strong signals attributed to the PCL crystal were well observed.

From the DSC instrument, the crystallization behaviors of marcoinitiator $[PEO\text{-}(OH)_4\text{-}PEO]_s$ and graft polymers PEO-*g*-PCL_4

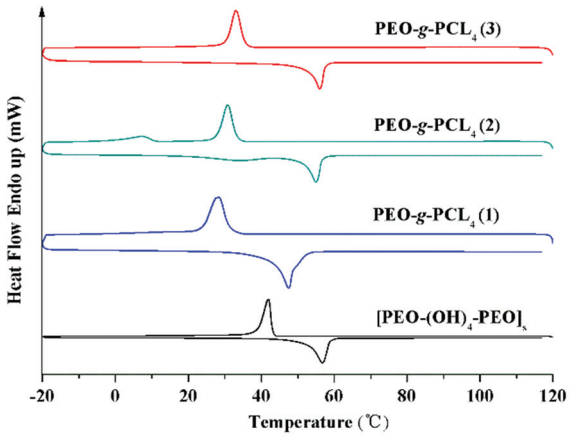

Fig. 10 DSC curves (10 °C min^{-1}) of the macroinitiator [PEO-$(OH)_4$-PEO]$_s$ and graft polymers PEO-*g*-PCL_4 in the cooling run and the second heating run.

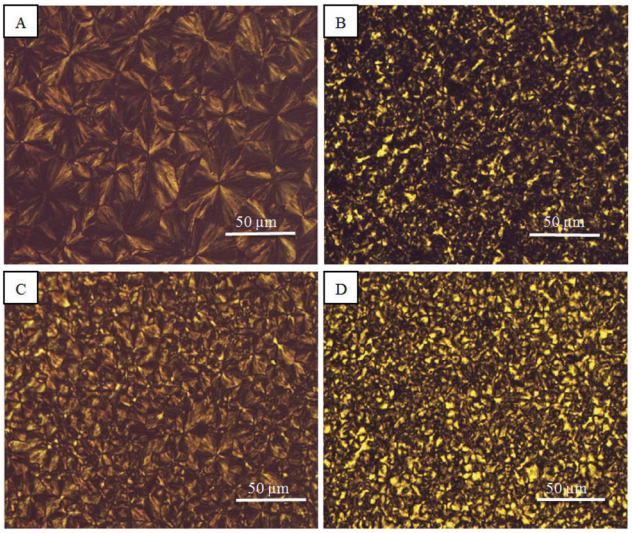

Fig. 11 The optical microscopy images of [PEO-$(OH)_4$-PEO]$_s$ (A), PEO-*g*-PCL_4 (**1**) (B), PEO-*g*-PCL_4 (**2**) (C), and PEO-*g*-PCL_4 (**3**) (D).

were also investigated (Fig. 10). In order to eliminate the effect of thermal history, the crystallization temperature (T_c) was obtained from the cooling run, and the melting temperature (T_m) was obtained from the second heating run. According to the literature, the T_m and T_c of the linear PCL were observed at 57.3 °C and 28.9 °C, while the T_m and T_c were observed at 59.5 °C and 37.8 °C, respectively.[65] Herein, for [PEO-$(OH)_4$-PEO]$_s$, the T_m and T_c were observed at 56.69 °C and 41.91 °C, respectively. After the PCL segment was introduced onto the PEO main chain, for the sample PEO-*g*-PCL_4 (**1**), the T_m and T_c were dramatically decreased to 47.45 °C and 28.16 °C. By combination with XRD results, we can conclude that the PEO and PCL segment formed the co-crystal structure and only one T_m or T_c was discriminated. However, when the content of the PCL segment was increased to 67.3% for sample PEO-*g*-PCL_4 (**2**), the crystalline structure of the PEO segment also disappeared and that of the PCL segment became the dominant part. The almost negligible T_m and T_c appeared at 34.70 °C and 7.41 °C were inferred as that of the PEO segment, while the increased and well discriminated T_m and T_c at 54.96 °C and 30.70 °C were ascribed to the PCL part, respectively. When the content of the PCL segment was further increased to 85.2% for sample PEO-*g*-PCL_4 (**3**), the T_m or T_c of the PCL segment was increased to 56.00 °C and 33.13 °C, respectively. Thus, all these DSC results were rather coincided with those from XRD patterns. Obviously, with the increase of the PCL length on side chains, the PEO main chain was surrounded and restricted, and the crystalline structure was transformed and dominated by the PCL part.

Finally, the detailed crystalline structure of graft polymers was also monitored and confirmed using the POM instrument. From Fig. 11, we could observe that the [PEO-$(OH)_4$-PEO]$_s$ formed the larger spherulite, while all the graft polymers formed the smaller spherulite. Especially, the more the PCL content designed into graft polymers (from 51.2% of PEO-*g*-PCL_4 (**1**) to 85.2% of PEO-*g*-PCL_4 (**3**)), the smaller the size of spherulite formed, which was rather accorded with the literature claiming that the PCL segment was usually crystallized at a relatively slow rate and tended to form a smaller crystalline structure.[66–68] The results obtained by the POM instrument further verified the conclusions drawn from the DSC and XRD instruments.

According to the literature,[69–74] for the copolymer of PCL-*b*-PEO, PEO-*b*-PCL-*b*-PEO or PCL-*b*-PEO-*b*-PCL with the simplest topology, it was reported that the crystallization behavior of these copolymers depends on the length of each block. For example, the PEO segment in PCL-*b*-PEO could still crystallize even when its weight fraction was only 14.0%. However, in this contribution, the signals corresponding to the crystallization of the PEO segment could no longer be discriminated by the above XRD, DSC and POM instruments when the weight fraction of the PEO segment was lowered to 14.8% (PEO-*g*-PCL_4 (**3**)). Obviously, all the above results confirmed that the architecture and compositions of copolymers actually have separate effects on their physical properties.

Conclusions

By combination of the ROP mechanism and Glaser coupling with thiol–yne addition reaction, the biodegradable and biocompatible amphiphilic graft polymers PEO-*g*-PCL_4 were successfully synthesized *via* the "grafting from" strategy. This novel versatile method can be further used to synthesize plenty of barbwire-like graft polymers by modulating the compositions of main chains and side chains. Also, by means of DSC, XRD, and POM instruments, the crystallization behavior of graft polymers PEO-*g*-PCL_4 was investigated and compared, and the results led to the conclusion that the architecture and compositions of copolymers could have separate effects on physical properties.

Acknowledgements

We appreciate the financial support of this research by the Natural Science Foundation of China (21004011, 50873093).

Notes and references

1 V. S. Trubetskoy, *Adv. Drug Delivery Rev.*, 1999, **37**, 81–88.
2 S. E. Stiriba, H. Kautz and H. Frey, *J. Am. Chem. Soc.*, 2002, **124**, 9698–9699.
3 M. Zhang, M. Drechsler and A. H. E. Muller, *Chem. Mater.*, 2004, **16**, 537–543.
4 R. Djalali, S. Y. Li and M. Schmidt, *Macromolecules*, 2002, **35**, 4282–4288.
5 L. H. He, J. Huang, Y. M. Chen, X. J. Xu and L. P. Liu, *Macromolecules*, 2005, **38**, 3845–3851.
6 N. Hadjichristidis, M. Pitsikalis, S. Pispas and H. Latrou, *Chem. Rev.*, 2001, **101**, 3747–3792.
7 S. J. Teertstra and M. Gauthier, *Prog. Polym. Sci.*, 2004, **29**, 277–327.
8 F. P. Yu, J. P. He, X. J. Wang, G. Z. Gao and Y. L. Yang, *J. Polym. Sci., Part A: Polym. Chem.*, 2007, **45**, 4013–4025.
9 A. X. Li, Z. J. Lu, Q. F. Zhou, F. Qiu and Y. L. Yang, *J. Polym. Sci., Part A: Polym. Chem.*, 2006, **44**, 3942–3946.
10 D. Uhrig and J. W. Mays, *Macromolecules*, 2002, **35**, 7182–7190.
11 X. Xiao, Y. G. Wu, M. H. Sun, J. J. Zhou, Z. S. Li, L. Bo and C. M. Chan, *J. Polym. Sci., Part A: Polym. Chem.*, 2008, **46**, 574–584.
12 P. Driva, D. J. Lohse and N. Hadjichristidis, *J. Polym. Sci., Part A: Polym. Chem.*, 2008, **46**, 1826–1842.
13 B. Helms, J. L. Mynar, C. J. Hawker and J. M. J. Frechet, *J. Am. Chem. Soc.*, 2004, **126**, 15020–15021.
14 Z. S. Bo and A. D. Schluter, *Chem. – Eur. J.*, 2000, **6**, 3235–3241.
15 T. T. Tang, J. Huang, B. Huang, G. W. Wang and J. L. Huang, *J. Polym. Sci., Part A: Polym. Chem.*, 2012, **50**, 5144–5150.
16 G. W. Wang, X. S. Fan and J. L. Huang, *J. Polym. Sci., Part A: Polym. Chem.*, 2010, **48**, 3797–3806.
17 Z. Y. Li, P. P. Li and J. L. Huang, *J. Polym. Sci., Part A: Polym. Chem.*, 2006, **44**, 4361–4371.
18 S. J. Teertstra and M. Gauthier, *Macromolecules*, 2007, **40**, 1657–1666.
19 G. Koutalas, D. J. Lohse and N. Hadjichristidis, *J. Polym. Sci., Part A: Polym. Chem.*, 2005, **43**, 4040–4049.
20 A. Hirao, H. Kawano and S. W. Ryu, *Polym. Adv. Technol.*, 2002, **13**, 275–284.
21 Y. G. Li, Y. Q. Zhang, D. Yang, Y. J. Li, J. H. Hu, C. Feng, S. J. Zhai, G. L. Lu and X. Y. Huang, *Macromolecules*, 2010, **43**, 262–270.
22 X. W. Xu and J. L. Huang, *J. Polym. Sci., Part A: Polym. Chem.*, 2006, **44**, 467–476.
23 H. Q. Xie and D. Xie, *Prog. Polym. Sci.*, 1999, **24**, 275–313.
24 R. Riva, S. Schmeits, C. Jerome, R. Jerome and P. Lecomte, *Macromolecules*, 2007, **40**, 796–803.
25 F. A. Plamper, S. Reinicke, M. Elomaa, H. Schmalz and H. Tenhu, *Macromolecules*, 2010, **43**, 2190–2203.
26 J. W. Mays, D. Uhrig, S. Gido, Y. Q. Zhu, R. Weidisch, H. Iatrou, N. Hadjichristidis, K. Hong, F. Beyer, R. Lach and M. Buschnakowski, *Macromol. Symp.*, 2004, **215**, 111–126.
27 H. Iatrou, J. W. Mays and N. Hadjichristidis, *Macromolecules*, 1998, **31**, 6697–6701.
28 D. Uhrig and J. W. Mays, *Macromolecules*, 2002, **35**, 7182–7190.
29 D. A. Herold, K. Keil and D. E. Bruns, *Biochem. Pharmacol.*, 1989, **38**, 73–76.
30 S. Jain and F. S. Bates, *Macromolecules*, 2004, **37**, 1511–1523.
31 C. X. Cheng, Y. Huang, R. P. Tang, E. Q. Chen and F. Xi, *Macromolecules*, 2005, **38**, 3044–3047.
32 P. Jannasch, *Macromolecules*, 2000, **33**, 8604–8610.
33 K. E. Uhrich, S. M. Cannizzaro, R. S. Langer and K. M. Shakesheff, *Chem. Rev.*, 1999, **99**, 3181–3198.
34 M. Vert, S. M. Li, G. Splenehauer and P. Guerin, *J. Mater. Sci.: Mater. Med.*, 1992, **3**, 432–446.
35 Y. N. Zhang, G. W. Wang and J. L. Huang, *J. Polym. Sci., Part A: Polym. Chem.*, 2010, **48**, 5974–5981.
36 G. W. Wang, X. L. Luo, C. Liu and J. L. Huang, *J. Polym. Sci., Part A: Polym. Chem.*, 2008, **46**, 2154–2166.
37 S. Binauld, C. J. Hawker, E. Fleury and E. Drockenmuller, *Angew. Chem., Int. Ed.*, 2009, **48**, 6654–6658.
38 P. Siemsen, R. C. Livingston and F. Diederich, *Angew. Chem., Int. Ed.*, 2000, **39**, 2632–2657.
39 T. Ogawa, *Prog. Polym. Sci.*, 1995, **20**, 943–985.
40 B. Hoffmann, D. Zanini, I. Ripoche, R. Burli and A. Vasella, *Helv. Chim. Acta*, 2001, **84**, 1862–1888.
41 Z. Li, Y. Q. Dong, M. Haussler, J. W. Y. Lam, Y. P. Dong, L. J. Wu, K. S. Wong and B. Z. Tang, *J. Phys. Chem. B*, 2006, **110**, 2302–2309.
42 K. Endo, *Adv. Polym. Sci.*, 2008, **217**, 121–183.
43 Y. N. Zhang, G. W. Wang and J. L. Huang, *Macromolecules*, 2010, **43**, 10343–10347.
44 B. Huang, X. S. Fan, G. W. Wang, Y. N. Zhang and J. L. Huang, *J. Polym. Sci., Part A: Polym. Chem.*, 2012, **50**, 2444–2451.
45 G. W. Wang, X. S. Fan and B. Hu, *Macromol. Rapid Commun.*, 2011, **32**, 1658–1663.
46 G. W. Wang, X. S. Fan and B. Hu, *Macromolecules*, 2012, **45**, 3779–3786.
47 X. S. Fan, T. T. Tang, K. Huang, G. W. Wang and J. L. Huang, *J. Polym. Sci., Part A: Polym. Chem.*, 2012, **50**, 3095–3103.
48 X. S. Fan, B. Huang, G. W. Wang and J. L. Huang, *Polymer*, 2012, **53**, 2890–2896.
49 G. W. Wang, B. Hu, X. S. Fan, Y. N. Zhang and J. L. Huang, *J. Polym. Sci., Part A: Polym. Chem.*, 2012, **50**, 2227–2235.
50 G. W. Wang, B. Hu and J. L. Huang, *Macromolecules*, 2010, **43**, 6939–6942.
51 O. Turunc and M. A. R. Meier, *J. Polym. Sci., Part A: Polym. Chem.*, 2012, **50**, 1689–1695.

52 L. X. Li, D. Zahner, Y. Su, C. Gruen, G. Davidson and P. A. Levkin, *Biomaterials*, 2012, **33**, 8160–8166.
53 S. Ye, N. B. Cramer, I. R. Smith, K. R. Voigt and C. N. Bowman, *Macromolecules*, 2011, **44**, 9084–9090.
54 H. Y. Park, C. J. Kloxin, T. F. Scott and C. N. Bowman, *Macromolecules*, 2010, **43**, 10188–10190.
55 C. Wang, P. F. Ren, X. J. Huang, J. A. Wu and Z. K. Xu, *Chem. Commun.*, 2011, **47**, 3930–3932.
56 R. F. Storey and J. W. Sherman, *Macromolecules*, 2002, **35**, 1504–1512.
57 C. He, J. Sun, T. Zhao, Z. Hong, X. Zhuang, X. Chen and X. Jing, *Biomacromolecules*, 2006, **7**, 252–258.
58 H. Takeshita, K. Fukumoto, T. Ohnishi, T. Ohkubo, M. Miya, K. Takenaka and T. Shiomi, *Polymer*, 2006, **47**, 8210–8218.
59 J. Z. Bei, J. M. Li, Z. F. Wang, J. C. Le and S. G. Wang, *Polym. Adv. Technol.*, 1997, **8**, 693–696.
60 B. Jeong, Y. H. Bae, D. S. Lee and S. W. Kim, *Nature*, 1997, **388**, 860–862.
61 S. Chen, R. Pieper, D. C. Webster and J. Singh, *Int. J. Pharm.*, 2005, **288**, 207–218.
62 L. Wang, J. L. Wang and C. M. Dong, *J. Polym. Sci., Part A: Polym. Chem.*, 2005, **43**, 4721–4730.
63 L. Chen, Y. S. Ni, X. C. Bian, X. Y. Qiu, X. L. Zhuang, X. S. Chen and X. B. Jiang, *Carbohydr. Polym.*, 2005, **60**, 103–109.
64 G. Maglio, G. Nese, M. Nuzzo and R. Palumbo, *Macromol. Rapid Commun.*, 2004, **25**, 1139–1144.
65 W. Z. Yuan, J. Y. Yuan, F. B. Zhang, X. M. Xie and C. Y. Pan, *Macromolecules*, 2007, **40**, 9094–9102.
66 S. Jiang, C. He, L. An, X. Chen and B. Jiang, *Macromol. Chem. Phys.*, 2004, **205**, 2229–2234.
67 C. He, J. Sun, C. Deng, T. Zhao, M. Deng, X. Chen and X. Jing, *Biomacromolecules*, 2004, **5**, 2042–2047.
68 T. Shiomi, K. Imai, K. Takenaka, H. Takeshita, H. Hayashi and Y. Tezuka, *Polymer*, 2001, **42**, 3233–3239.
69 C. L. He, J. R. Sun, T. Zhao, Z. K. Hong, X. L. Zhuang, X. S. Chen and X. B. Jing, *Biomacromolecules*, 2006, **7**, 252–258.
70 C. L. He, J. R. Sun, J. Ma, X. S. Chen and X. B. Jing, *Biomacromolecules*, 2006, **7**, 3482–3489.
71 C. L. He, J. R. Sun, C. Deng, T. Zhao, M. X. Deng, X. S. Chen and X. B. Jing, *Biomacromolecules*, 2004, **5**, 2042–2047.
72 T. Shiomi, K. Imai, K. Takenaka, H. Takeshita, H. Hayashi and Y. Tezuka, *Polymer*, 2001, **42**, 3233–3239.
73 Z. H. Gan, J. Zhang and B. Z. Jiang, *J. Appl. Polym. Sci.*, 1997, **63**, 1793–1804.
74 B. Bogdanov, A. Vidts and E. Schacht, *Macromolecules*, 1999, **32**, 726–731.